Journal of Alloys and Compounds 495 (2010) 352–355

Contents lists available at ScienceDirect

Journal of Alloys and Compounds

journal homepage: www.elsevier.com/locate/jallcom

Estimation of heat production during high pressure torsion of Cu-based metallic glass

Sándor Hóbor[a], Zsolt Kovács[a,b], Ádám Révész[a,*]

[a] Department of Materials Physics, Eötvös University, Budapest, H-1518, P.O.B. 32, Budapest, Hungary
[b] School of Electrical, Electronic & Mechanical Engineering, University College Dublin, Belfield, Dublin 4, Ireland

ARTICLE INFO

Article history:
Received 3 July 2008
Received in revised form 8 October 2009
Accepted 9 October 2009
Available online 20 October 2009

Keywords:
Metallic glasses
Heat conduction
Thermodynamic modeling
Microstructure
Nanostructured materials

ABSTRACT

In order to estimate the temperature rise generated by the extreme shear during high pressure torsion deformation, a simple model based on the one-dimension heat-conduction equation was proposed. Calculations have shown that the average temperature in the sample can slightly exceed the glass transition temperature above a critical strain. The experimentally obtained shear dependent microstructure and morphology of an amorphous $Cu_{60}Zr_{30}Ti_{10}$ alloy are consistent with the calculated temperature profiles.

1. Introduction

Severe plastic deformation (SPD) techniques are used over the last several decades to refine the microstructure or increase the alloying content beyond the equilibrium limit of crystalline alloys. One of the most frequently used SPD techniques for producing bulk nanocrystalline samples is high pressure torsion (HPT) [1,2], in which disk-shaped samples are strained by torsion under several GPa of pressure between two anvils. Recently the HPT method has also been successfully applied for amorphous materials to produce massive samples by consolidation of small pieces (ribbons, flakes) at room temperature and to enhance the mechanical properties of bulk metallic glasses (BMGs) by introducing a second nanocrystalline phase [3–9]. It is well-known, that room-temperature plastic deformation of BMGs is extremely localized in very thin shear bands, with a thickness of ~10 nm [10]. Local heating around these shear bands may rise the temperature high enough to induce nanocrystals thermally [11]. However as the temperature of the overall BMG sample exceeds the glass transition temperature (T_g) the transition takes place in the deformation from inhomogeneous to homogenous viscous flow [12].

In the present work a simple model based on heat conduction estimating the temperature rise generated by the extensive shear during HPT-deformation is proposed. As an example, it is demonstrated that the experimentally observed morphological and microstructural features of a $Cu_{60}Zr_{30}Ti_{10}$ amorphous alloy subjected to HPT-deformation can be explained by the calculated temperature profiles.

2. Numerical calculations

In crystalline materials, plastic deformation leads to the homogenization of material parameters due to the gradient plasticity terms originating from finite crystal size and dislocation hardening [13,14]. As metallic glasses lack both gradient terms, homogenization of the material parameters only occurs only by the relaxation of deformation induced thermal differences. Accordingly, the estimation of the temperature rise during HPT-deformation can be estimated from the conduction of heat generated by the extensive shear deformation. Fig. 1 shows the schematic image of an unconstrained HPT-device with a disk-shaped sample placed between two stainless steel anvils. The accumulated shear strain during the HPT process at a radius r can be represented by

$$\varepsilon(r,t) = \frac{2\pi N r}{L} = \frac{\omega r}{L} t, \quad (1)$$

where N, L, t and ω are the number of rotations, the thickness of the disk, the time and the angular speed, respectively [2]. In order to obtain the temperature along the diameter, the one-dimensional heat-conduction equation with a source term was solved numeri-

* Corresponding author. Tel.: +36 1 372 28 23; fax: +36 1 372 28 11.
E-mail address: reveszadam@ludens.elte.hu (Á. Révész).

0925-8388/$ – see front matter © 2009 Elsevier B.V. All rights reserved.
doi:10.1016/j.jallcom.2009.10.056

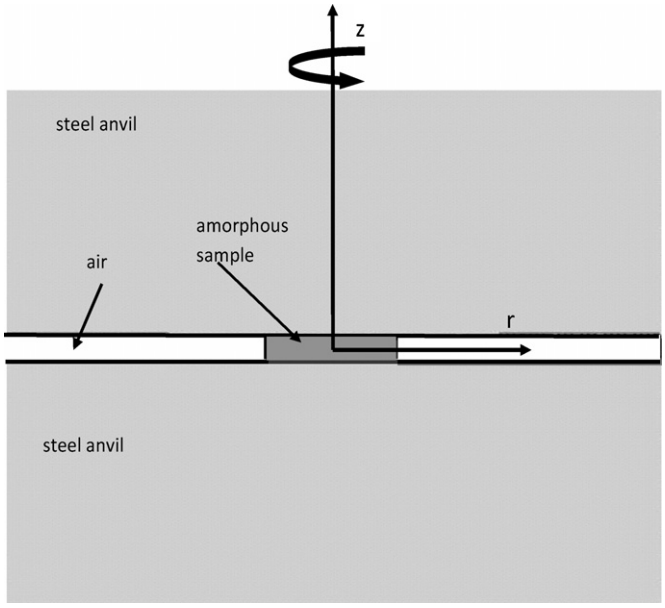

Fig. 1. Schematic illustration of the high pressure torsion (HPT) device and the deformed disk-shaped sample.

cally:

$$c\rho\frac{\partial T(z,r,t)}{\partial t} - k\left(\frac{\partial^2 T(z,r,t)}{\partial z^2}\right) = S(z,r,t), \tag{2}$$

where c, ρ and k are the heat capacity, the density and the heat conductivity, respectively. Due to the relative small sample thickness and the poor thermal conductivity of metallic glasses, the one-dimensional equation can yield satisfactory result with r as a simple parameter. The source term, $S(z, r, t)$ is zero in the steel anvils and can be given in the metallic glass as follows:

$$S(z,r,t) = \begin{cases} \beta\sigma\dfrac{d\varepsilon}{dt} & \text{if} \quad T < T_g \\ \beta\eta\left(\dfrac{d\varepsilon}{dt}\right)^2 & \text{if} \quad T > T_g, \end{cases} \tag{3}$$

where β, η and ε are the fraction of plastic work converted to thermoplastic heating (chosen as 0.5 [15]), the viscosity and the shear strain, respectively. ε can be calculated from Eq. (1), and the viscosity above T_g was estimated from the Vogel–Fulcher equation

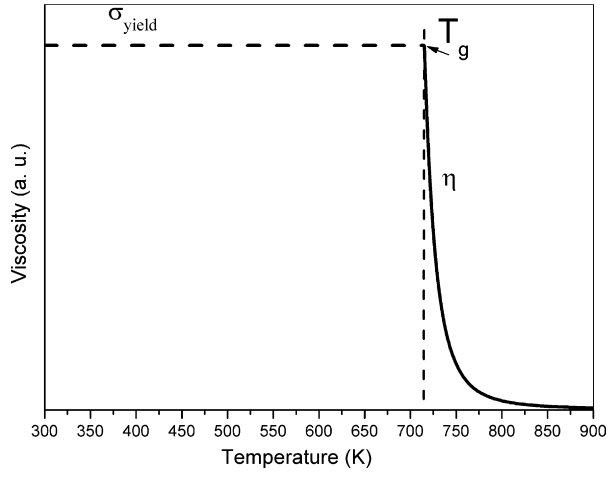

Fig. 2. Temperature dependence of the viscosity (η) according to the Vogel–Fulcher equation.

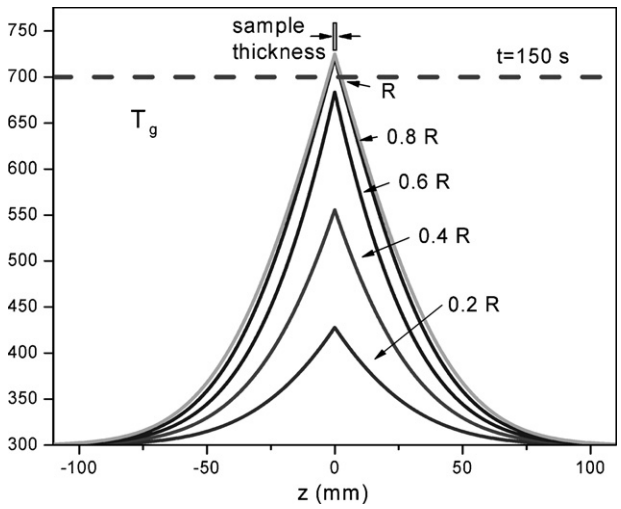

Fig. 3. Temperature profiles obtained from the heat-conduction equation (Eq. (2)) at different r values perpendicular to the surface of the disk in the steel anvils.

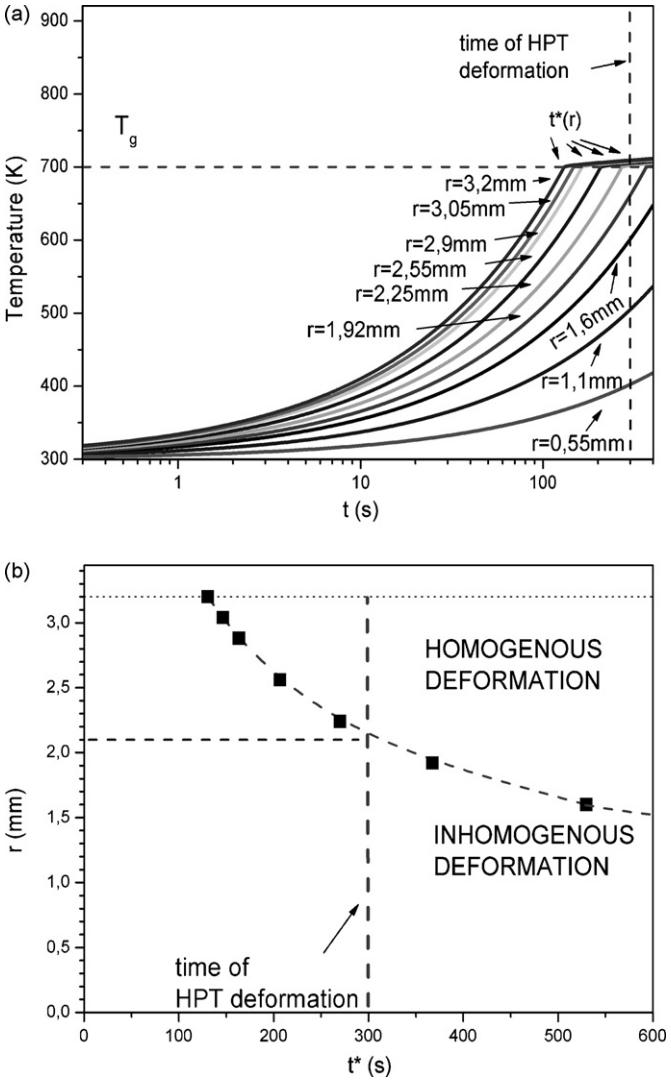

Fig. 4. (a) Temperature evolution as a function of the processing time for different distances from the rotation axis. The characteristic time (t^*), needed to reach T_g is also indicated. (b) The characteristic time (t^*) values for different radial distances (r).

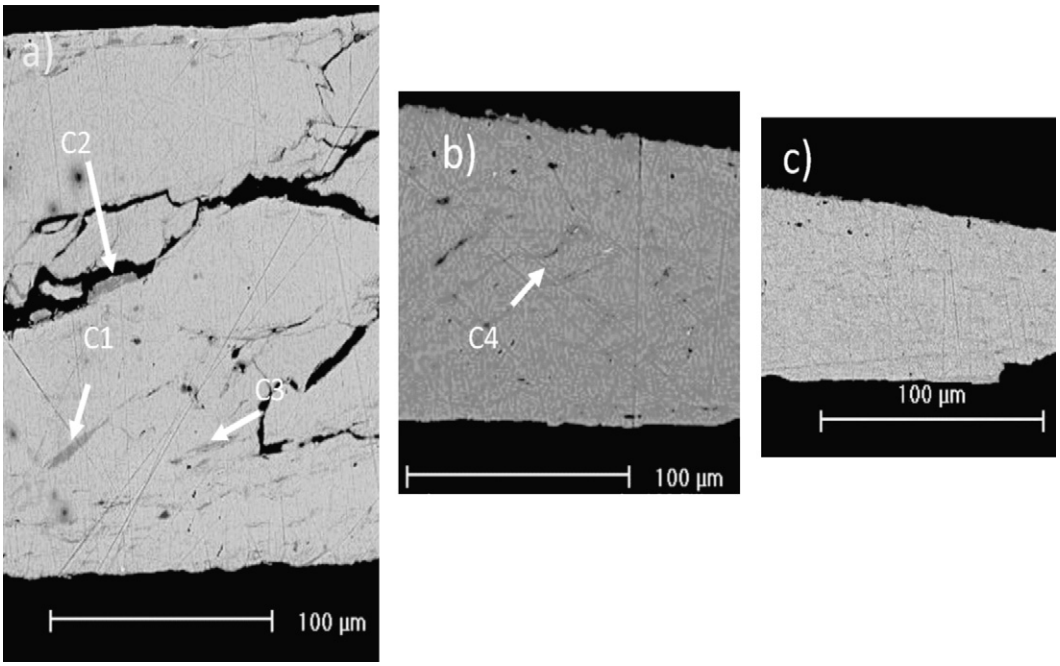

Fig. 5. SEM BSE images taken at different distances from the rotation axis of the cross-section of the HPT disk (a) at the central part (b) at larger distance from the center (c) at the perimeter.

[16]:

$$\eta = \eta_0 e^{BT_{vf}/(T-T_{vf})}, \quad (4)$$

where η_0 and B are Vogel–Fulcher constants. The temperature dependence of the viscosity (η) is plotted in Fig. 2. In the calculations the following material parameters were used which are typical for a Cu-based metallic glass i.e. $k = 7.7\,W\,m^{-1}\,K^{-1}$, $c = 420\,J\,kg^{-1}\,K^{-1}$, $\rho = 6125\,kg\,m^{-3}$ [11], $T_g = 700\,K$ [17], $T_{vf} = 610\,K$. The constants η_0 and B were chosen ($\eta_0 = 591\,Pa$, $B = 1.1$) so: $\sigma_{yield} = 1.2\,GPa$ at T_g, characteristic value for metallic glasses [18]. The initial temperature in the calculation was 300 K.

In order to take into account the influence of the heat conduction through the steel anvils on the evolution of the temperature, Eq. (2) was solved for one-dimensional sections parallel to axis z at different r distances from the rotation axis (see Fig. 1). The thermal parameters chosen for stainless steel are: $k = 18\,W\,m^{-1}\,K^{-1}$, $c = 460\,J\,kg^{-1}\,K^{-1}$, $\rho = 7800\,kg\,m^{-3}$. The corresponding temperature profiles obtained at $t = 150\,s$ are shown in Fig. 3. As seen, the temperature can increase significantly in the HPT sample, although, the majority of the deformation induced heat is conducted by the steel anvils. Once the temperature exceeds the T_g, the slope of the temperature profiles drops considerably (see Fig. 4a) due to the strong temperature dependence of the viscosity. Thereafter, the temperature shows only a small increase (~10 K) and remains well below the liquidus temperature ($T_l = 1192\,K$ [19]) until the HPT process is complete. Based on the temperature evolution in the HPT sample, the characteristic time $t^*(r)$ required to reach T_g is plotted in Fig. 4b for different r distances. Here we note that the characteristics of the temperature profiles mainly depend on the heat conductivity of the steel anvils and only slightly on material parameters of the BMG.

According to the aforementioned model, the temperature exceeds T_g only in the outer part of the HPT disk in the range of $2.2\,mm < r < 3.2\,mm$ during the full length (300 s) of the deformation process, however, the temperature of the inner regions remains practically below T_g. As a consequence, the amorphous disk can be divided into two regions (see Fig. 4b), i.e. in the central region the deformation mode is inhomogeneous while it turns to homogenous in the outer part after $t^*(r)$. In a more realistic approach, when heat conduction in both z and r direction is calculated simultaneously, the curve seen in Fig. 4b becomes steeper, yielding the temperature to exceed T_g in larger volumes of the sample. This is going to be examined in detail in an upcoming paper [20].

The obtained significantly higher temperature rise in metallic glasses (see Figs. 3 and 4) compared to crystalline materials (20–140 K [21,22]) is related to the significantly higher yield stress [12]. In order to demonstrate the effect of the calculated shear dependent temperature rise, the deformation dependence of the morphology, microstructure and thermal behavior of a $Cu_{60}Zr_{30}Ti_{10}$ HPT-deformed amorphous alloy was investigated thoroughly in a recent paper [17]. In the following only the main points will be highlighted.

3. Experimental demonstration

Backscattered scanning electron microscope (SEM BSE, Phillips XL 30) images taken at different points on the cross-section of the HPT sample can visualize the most important microstructural changes associated with the severe shear deformation (Fig. 5a–c). Although the amorphous alloy exhibits featureless, homogeneous microstructure (not shown here), the morphology of the HPT disk is distinctly diverse. As seen, in the central region several elongated dark gray blocks (C1–C3) with a length of around 15–20 μm are homogeneously dispersed in the matrix (Fig. 5a). Quantitative elemental analysis taken at several points confirmed that the composition of the contrastless matrix is equal to that of the as-quenched alloy ($Cu_{60}Zr_{30}Ti_{10}$), however, the average composition of the C1–C3 blocks is slightly different ($Cu_{62}Zr_{20}Ti_{18}$). At larger distances from the center, the disk shows transient microstructure (Fig. 5b), i.e. with increasing radius the size and density of the visible elongated blocks decrease and further they disappear. The maximum length of these particles decreases down to 5 μm, while their composition remains practically unchanged. As seen in Fig. 5c, the perimeter exhibits only contrastless homogeneous microstructure without any detectable crystalline blocks with an average composition of $Cu_{60}Zr_{30}Ti_{10}$. Supplementary continuous heating

calorimetric measurements revealed that the shear deformation results in a less pronounced glass transition and simultaneously in a significant drop of the total crystallization enthalpy [17].

Based on the numerical calculations, it is supposed that the first stage of the deformation process is dominated by the formation of randomly distributed nuclei in the amorphous matrix. Subsequently, as the temperature exceeds T_g in the outer region, the growth and the coalescence of these nanocrystals in the viscous glass are limited by the persistent homogeneous shear, resulting in a relatively homogeneous microstructure (Fig. 5c). On contrary, the inner part of the disk is dominated by inhomogeneous deformation for a longer time, resulting in the formation of large crystalline blocks (see Fig. 5a).

4. Conclusions

Numerical calculations using a model based on one-dimensional heat-conduction equation with heat conduction through the steel anvils showed that there exists a necessary characteristic time for the temperature to reach T_g, which varies significantly with the magnitude of shear strain and strain rate. Once T_g is reached the slope of the temperature profiles decreases considerably, corresponding to the drastic decrease of mechanical energy input. In accordance with the radial dependent shear deformation, the $Cu_{60}Zr_{30}Ti_{10}$ sample exhibits gradient microstructure, i.e. large, deformed crystalline blocks in the interior, while homogeneously dispersed nanocrystals embedded in the amorphous matrix at the perimeter.

Acknowledgements

We appreciate the support of the Hungarian Scientific Research Fund under grant Nos. 67893 and 67692. Á.R. is indebted for the Bolyai Scholarship of the Hungarian Academy of Sciences. The authors are grateful to Dr. L.K. Varga for providing the amorphous ribbon, to Dr. A. Zhilyaev for the HPT disk and to Dr. P.J. Szabó for the SEM study.

References

[1] R.Z. Valiev, R.K. Islamgaliev, I.V. Alexandrov, Prog. Mater. Sci. 45 (2000) 103.
[2] A.P. Zhilyaev, T.G. Langdon, Prog. Mater. Sci. 53 (2008) 893.
[3] J. Sort, D.C. Ile, A.P. Zhilyaev, A. Concustell, T. Czeppe, M. Stoica, S. Suriñach, J. Eckert, M.D. Baró, Scripta Mater. 50 (2004) 1221.
[4] N. Boucharat, R. Hebert, H. Rösner, R. Valiev, G. Wilde, Scripta Mater. 53 (2005) 823.
[5] Zs. Kovács, P. Henits, A.P. Zhilyaev, Á. Révész, Scripta Mater. 54 (2006) 1733.
[6] Á. Révész, S. Hóbor, P.J. Szabó, A.P. Zhilyaev, Zs. Kovács, Mater. Sci. Eng. A 460–461 (2007) 459.
[7] T. Czeppe, G.F. Korznikova, P. Ochin, A.V. Korznikov, N.Q. Chinh, A. Sypień, J. Phys. 98 (2008) 062035.
[8] R.J. Herbert, N. Boucharat, J.H. Perepezko, H. Rösner, G. Wilde, J. Alloys Compd. 434–435 (2007) 252.
[9] P. Henits, Á. Révész, A.P. Zhilyaev, Zs. Kovács, J. Alloys Compd. 461 (2008) 195.
[10] H. Chen, Y. He, G.J. Shiflet, S.J. Poon, Nature 367 (1994) 541.
[11] J.J. Lewandowski, A.L. Greer, Nat. Mater. 5 (2006) 15.
[12] C.A. Schuh, T.C. Hufnagel, U. Ramamurty, Acta Mater. 55 (2007) 4067.
[13] Y. Estrin, A. Molotnikov, C.H.J. Davies, R. Lapovok, J. Mech. Phys. Solids 56 (2008) 1186.
[14] C. Xu, Z. Horita, T.G. Langdon, Acta Mater. 56 (2008) 5168.
[15] P. Rosakis, A. Rosakis, A.J. Ravichandran, G. Hodowany, J. Mech. Phys. Solids 48 (2000) 581.
[16] G.S. Fulcher, J. Am. Ceram. Soc. 6 (1925) 339.
[17] S. Hóbor, Á. Révész, P.J. Szabó, A.P. Zhilyaev, V. Kovács Kis, J.L. Lábár, Zs. Kovács, J. Appl. Phys. 104 (2008) 033525.
[18] A. Inoue, W. Zhang, T. Zhang, K. Kurosaka, Acta Mater. 49 (2001) 2645.
[19] A. Concustell, M. Zielinska, Á. Révész, L.K. Varga, S. Suriñach, M.D. Baró, Intermetallics 12 (2004) 1063.
[20] S. Hóbor, Zs. Kovács, Á. Révész, in preparation.
[21] Y. Todaka, M. Umemoto, A. Yamazaki, J. Sasaki, K. Tsuchiya, Mater. Trans. 49 (2008) 7.
[22] A.P. Zhilyaev, J.M. García-Infanta, F. Carreño, T.G. Langdon, O.A. Ruano, Scripta Mater. 57 (2007) 763.